

# Analysis of the Relationship of U.S. Droughts with SST and Soil Moisture: Distinguishing the Time Scale of Droughts

RENGUANG WU

*Center for Ocean–Land–Atmosphere Studies, Calverton, Maryland*

JAMES L. KINTER III

*Center for Ocean–Land–Atmosphere Studies, Calverton, Maryland, and Department of Atmospheric, Ocean and Earth Sciences, George Mason University, Fairfax, Virginia*

(Manuscript received 16 September 2008, in final form 8 December 2008)

## ABSTRACT

The impacts of droughts depend on how long droughts persist and the reasons why droughts extend to different time scales may be different. **The present study distinguishes the time scale of droughts based on the standardized precipitation index and analyzes the relationship of boreal summer U.S. droughts with sea surface temperature (SST) and soil moisture.** It is found that the roles of remote SST forcing and local soil moisture differ significantly for long-term and short-term droughts in the U.S. Great Plains and Southwest. For short-term droughts ( $\leq 3$  months), simultaneous remote SST forcing plays an important role with an additional contribution from soil moisture. For medium-term and long-term droughts ( $\geq 6$  months), both simultaneous and antecedent SST forcing contribute to droughts, and the soil moisture is important for the persistence of droughts through a positive feedback to precipitation. The antecedent remote SST forcing contributes to droughts through soil moisture and evaporation changes. The tropical Pacific SST is the dominant remote forcing for U.S. droughts. The most notable impacts of the tropical Pacific SST are found in the Southwest with extensions to the Great Plains. Tropical Indian Ocean SST forcing has a notable influence on medium-term and long-term U.S. droughts. The relationships between tropical Indian and Pacific Ocean SST and boreal summer U.S. droughts have undergone obvious long-term changes, especially for the Great Plains droughts.

## 1. Introduction

Droughts and floods are extreme climate events that can cause substantial damage to the environment, economic losses in various sectors, damage to infrastructure, and even loss of life or livelihood. It is important to understand the causes, and thereby improve predictions, of droughts and floods. The continental United States has experienced several severe droughts in recorded history and there is evidence of large and prolonged droughts in the paleoclimatic record. Considerable effort has been made to understand the factors influencing U.S. droughts (e.g., Namias 1991; Trenberth et al. 1988; Trenberth and Branstator 1992; Piechota and Dracup 1996; Trenberth and Guillemot 1996; Mo et al. 1997; Dai et al.

1998; Rajagopalan et al. 2000; Hoerling and Kumar 2003; Schubert et al. 2004a,b; Andreadis et al. 2005; Seager et al. 2005; Seager 2007; Schubert et al. 2008; Mo and Schemm 2008). Previous studies have significantly improved our understanding of the occurrence of U.S. droughts.

The occurrence of U.S. drought has been linked to, among other factors, anomalous sea surface temperature (SST). In particular, many studies have demonstrated that droughts over the United States are associated with a cold eastern tropical Pacific (Piechota and Dracup 1996; Trenberth and Guillemot 1996; Ting and Wang 1997; Rajagopalan et al. 2000; Hoerling and Kumar 2003; Schubert et al. 2004a,b; Seager et al. 2005, 2008; Seager 2007; Schubert et al. 2008; Mo and Schemm 2008). Piechota and Dracup (1996) found a strong relationship between El Niño and extreme drought years in the Pacific Northwest, and dry conditions occur consistently in the southern United States during La Niña years. Hoerling and Kumar (2003) demonstrated the important

---

*Corresponding author address:* Renguang Wu, COLA, IGES, 4041 Powder Mill Road, Suite 302, Calverton, MD 20705.  
E-mail: renguang@cola.iges.org

contribution of persistent cold SST in the eastern tropical Pacific and warm SST in the western tropical Pacific–Indian Ocean to the 1998–2003 drought spanning the United States, southern Europe, and southwestern Asia. Schubert et al. (2004a,b) indicated that a primary cause for the 1930s persistent drought in the United States was the anomalously cold tropical Pacific SST. Seager et al. (2005) showed that persistent droughts during the 1930s and 1950s and the period of anomalously wet (pluvial) climate in the 1990s were at least, in part, forced by persistent variations of tropical Pacific SST.

Studies have indicated the contribution of SST anomalies in other regions to U.S. droughts, such as the midlatitude North Pacific (Namias 1991; Barlow et al. 2001; Hu and Huang 2007; Mo and Schemm 2008; Seager et al. 2008; White et al. 2008) and the tropical North Atlantic Ocean (Schubert et al. 2004a; Seager 2007). A warm North Pacific corresponds to droughts over the Southwest (Barlow et al. 2001; Mo and Schemm 2008). A cold tropical North Atlantic is associated with droughts over the Great Plains (Schubert et al. 2004b). Seager et al. (2005) suggested that ocean temperature variations outside of the tropical Pacific can act to strengthen the droughts and pluvials in the United States. Note that warm (cold) SST anomalies in the central-eastern tropical Pacific SST are often accompanied by warm (cold) SST anomalies in the subtropical North Atlantic and tropical Indian Ocean and cold (warm) SST anomalies in the midlatitude North Pacific owing to the “atmospheric bridge” (Klein et al. 1999; Alexander et al. 2002). Thus, the relationship of U.S. droughts with SST in these regions as revealed by correlation analysis may not be independent of that with SST in the tropical eastern Pacific.

The physical mechanisms connecting SST and U.S. droughts have been investigated in previous studies (Namias 1955; Chang and Wallace 1987; Trenberth and Guillemot 1996; Schubert et al. 2004b, 2008; Seager et al. 2005, 2008; Seager 2007). The Pacific SST impacts on summer droughts over the United States are accomplished through modifying the planetary waves and, hence, the Pacific storm tracks (Namias 1955; Schubert et al. 2004b, 2008). Tropical Pacific SST anomalies force changes in the subtropical jets, transient eddies, and the eddy-driven mean meridional circulation, and these changes generate anomalous subsidence and reduce moisture convergence over the United States (Seager et al. 2005; Seager 2007). The Atlantic SST anomalies force changes in the Bermuda high and low-level moisture flux into the U.S. continent (Schubert et al. 2004b, 2008).

Another important factor for droughts is a positive soil moisture–precipitation feedback. Initial soil moisture anomalies induced by precipitation variations associated with atmospheric circulation changes can positively

feedback on the succeeding precipitation, thus prolonging droughts (Findell and Eltahir 1997; Eltahir 1998; Pal and Eltahir 2001). The role of the soil moisture feedback in the occurrence of U.S. droughts has been shown in numerous studies (e.g., Oglesby and Erickson 1989; Trenberth and Branstator 1992; Atlas et al. 1993; Lyon and Dole 1995; Pan et al. 1995; Giorgi et al. 1996; Trenberth and Guillemot 1996; Paegle et al. 1996; Findell and Eltahir 1997; Fennessy and Shukla, 1999; Hong and Kalnay 2000; Pal and Eltahir 2001; Dirmeyer et al. 2003; Schubert et al. 2004b; Seager et al. 2005; Wu et al. 2006; Conil et al. 2007; Seager 2007; Mo and Schemm 2008). Pal and Eltahir (2001) suggested the importance of the positive soil moisture–precipitation feedback mechanism for the persistence of the Midwest U.S. drought into the summer. Findell and Eltahir (1997) identified a significant correlation between an initial soil moisture condition and the subsequent rainfall during the summer months based on observations in Illinois. This correlation suggests the likelihood of a physical feedback mechanism linking early summer soil moisture with subsequent precipitation. The role of the soil moisture feedback in extending drought from winter into summer was also indicated in Seager et al. (2005) and Seager (2007). Schubert et al. (2004b) showed that interactions between the atmosphere and land surface increased the severity of the 1930s drought.

The relationship between U.S. drought and SST forcing may also change with time (Cole and Cook 1998; Rajagopalan et al. 2000; Hu and Feng 2001; White et al. 2008). Cole and Cook (1998) found that the influence of El Niño and the Southern Oscillation (ENSO) on the U.S. drought has varied substantially over the past 130 years. The ENSO influence was more extensive before ~1910 than in later periods. From ~1910 to 1965, droughts associated with ENSO weakened in most regions but intensified in the Southwest. In the mid-Atlantic, ENSO warm extremes were correlated significantly with drier conditions. In the most recent decades, ENSO cold extremes are linked to Southwest droughts that penetrate northeastward and to significant mid-Atlantic anomalies of opposite sign. Rajagopalan et al. (2000) showed that the ENSO–summer U.S. drought teleconnection has changed in both its location and intensity. During the first three decades of the twentieth century, summer drought teleconnections linked to ENSO were strongest in the southern regions of Texas, with extensions into regions of the Midwest. From the 1930s through the 1950s the drought teleconnection pattern extended into southern Arizona. The next three decades showed weak drought teleconnections with ENSO over southern Texas and Arizona, with a clear shift to the western United States and southern California.

While previous studies have demonstrated the role of SST forcing and soil moisture in the occurrence of U.S. droughts, controversy can be found in the literature. The controversy arises because of the dependence of the results on event-to-event variations and differences among models used to simulate the relationships. The present study focuses on the statistically significant relationship between U.S. drought and SST forcing and the dependence of soil moisture feedback on the time scale of droughts.

The present study distinguishes droughts at different time scales. The importance of considering the droughts at different time scales has been pointed out in previous studies (e.g., López-Moreno and Vicente-Serrano 2008). We focus on time scales because, not only the impacts of drought depend on the time scale, but also the causes of droughts at different time scales could be different. The relative roles of SST forcing and land surface feedback can be different for long-term and short-term droughts. Thus, it is necessary to distinguish the time scale of droughts for a better understanding of the causes for droughts. Droughts can occur throughout the year. In this study, we focus on summer droughts with the purpose of demonstrating how the antecedent SST and soil moisture feedback contribute to droughts. In most of the Great Plains and Southwest, the percentage of precipitation is largest in summer and thus the impacts of summer droughts may be relatively large.

The main subject of this study is to investigate the relationship of U.S. summer droughts with SST and soil moisture for different drought time scales. We are interested in determining 1) where SST has the most significant relationship with the U.S. summer droughts, 2) where summer droughts are mostly influenced by remote SST forcing, and 3) the role of soil moisture in droughts. Another matter of interest for this study is the long-term change in the relationship between droughts and SST forcing. In the following, we first describe the datasets used in the present study (section 2). The relationship between the Palmer Drought Severity Index (PDSI) and the standard precipitation index (SPI) will be briefly discussed in section 3. Then, we analyze the correlation of SST with Great Plains drought, soil moisture, and surface evaporation (section 4). This is followed by analysis of the relationship of U.S. summer droughts with ENSO (section 5). The long-term changes in the SST–drought relationship will be documented in section 6. Summary and discussions will be given in section 7.

## 2. Datasets

### a. Drought indices

To characterize drought, we use both the Palmer Drought Severity Index and the standard precipitation

index for 344 U.S. climate divisions over the period 1895–2007. The PDSI developed by Palmer (1965) is widely used as an indicator of long-term drought. The SPI designed by McKee et al. (1993) can be defined for different time scales (see below). The SPI indices at different time scales are denoted by the number of months following SPI. For example, SPI06 refers to SPI at the 6-month time scale. The monthly PDSI and SPI values were obtained from the National Climatic Data Center (NCDC). For more information, refer to <http://www1.ncdc.noaa.gov/pub/data/cirs/drought.README>.

The PDSI is based on a water balance model. There are limitations with the PDSI that must be acknowledged in its use (Alley 1984; McKee et al. 1995; Kogan 1995). The PDSI is not as good for short-term drought. It is not well suited for mountainous regions and during winter months because of the assumption that all precipitation is rain. The weighting factors in the algorithm calculating the PDSI were empirically derived from a limited amount of data regardless of the climate in which it is used (Wells et al. 2004). PDSI can be slow to respond to developing and diminishing droughts (Hayes et al. 1999). PDSI is not spatially comparable across the contiguous United States (Alley 1984; Guttman et al. 1992; Guttman 1998). The severe/extreme values of the PDSI occur too frequently (Wells et al. 2004).

Recently, Wells et al. (2004) presented a self-calibrating PDSI for which empirical constants and weighting factors in the PDSI computation are calibrated to the local characteristics. The self-calibrating PDSI significantly improves the spatial comparability and reduces extreme dry and wet events to approximately 2% of the time locally. Comparison shows that the original PDSI and the self-calibrating PDSI are locally well correlated with very similar temporal behavior (Wells et al. 2004; van der Schrier et al. 2006). The point-to-point correlation over vast areas of the United States is up to or in excess of 0.9 (van der Schrier et al. 2006). We have recalculated the correlation (shown in Figs. 2 and 6 below) using the self-calibrating PDSI. In comparison, the correlation distribution is very similar to that using the original PDSI though there are some differences in magnitude of the correlation coefficient. In the present study, we show results using the original PDSI.

The SPI is based solely on the probability of precipitation for a given time period. For example, to obtain SPI06, first a time series is constructed by averaging precipitation from five months before to the current month. Then a transformation from a Pearson Type III distribution function to a normal distribution function is performed on the time series. After that, the SPI06 value is determined from the transformed time series. Other distributions such as gamma, lognormal, and beta can

also be used in calculating the SPI. The results are essentially equivalent (Guttman 1998, 1999). For the methods of calculating the SPI, refer to L6pes-Moreno and Vicente-Serrano (2008).

The SPI is a simpler measure of drought than the PDSI. The SPI considers only precipitation, while the PDSI is a water balance index that considers water supply (precipitation), demand (evapotranspiration), and loss (runoff). The SPI index varies between  $-3$  (anomalously dry) and  $3$  (anomalously wet); the more the index value departs from zero, the drier or wetter an event lasting six months (for SPI06) is when compared to the long-term climatology. The index allows for comparison of precipitation observations at different locations with markedly different climates; an index value at one location expresses the same relative departure from median conditions at one location as at another location. A key feature of the SPI is the flexibility to measure drought at different time scales, which allows separating and estimating contributions to a specific drought event at different time scales.

#### b. *Soil moisture*

The present study uses *monthly soil moisture*, evaporation, and river runoff for 344 U.S. climate divisions. The soil moisture is estimated by a one-layer hydrological model (Huang et al. 1996; van den Dool et al. 2003; Fan and van den Dool 2004). The model takes observed precipitation and temperature and calculates soil moisture, evaporation, and runoff. These data cover the period from 1932 to 2005 and are obtained from the Climate Prediction Center (CPC) (see <ftp://ftp.cpc.ncep.noaa.gov/wd51yf/us/>).

Observations at 19 soil moisture stations in Illinois are used in the present study mainly for validating the soil moisture–drought relationship. The average soil moisture for the 19 stations is formed and then the monthly mean is constructed. The observations cover the period from 1981 to June 2004. The present study uses the data from January 1984 to exclude the first three years during which the variability is smaller than the rest of the period. The Illinois soil moisture data (Hollinger and Isard 1994) were obtained from the Global Soil Moisture Data Bank of Robock et al. (2000) (see [http://climate.envsci.Rutgers.edu/soil\\_moisture/illinois.html](http://climate.envsci.Rutgers.edu/soil_moisture/illinois.html)).

Monthly mean soil moisture from the Variable Infiltration Capacity (VIC) model (Maurer et al. 2002) is also used in the present analysis to confirm the soil moisture–drought relationship. VIC is a macroscale hydrological model that balances both surface energy and water. The VIC model is forced with observed precipitation and temperature along with winds taken from atmospheric reanalysis (Kalnay et al. 1996). The other meteorological and radiation variables used to force the model are derived based on empirical relationships relating these

variables to precipitation and temperature. VIC provides soil moisture at three layers with a spatial resolution of  $1/8^\circ$  and covering the period 1950–2000. The VIC model soil moisture data were obtained from the University of Washington (see [ftp://ftp.hydro.washington.edu/pub/HYDRO/data/VIC\\_retrospective/](ftp://ftp.hydro.washington.edu/pub/HYDRO/data/VIC_retrospective/)).

#### c. *SST*

The present study uses the extended reconstruction of monthly mean SST version 2 (ERSST2) for the period 1854–2005 (Smith and Reynolds 2004). This SST dataset has a spatial resolution of  $2^\circ$ . The ERSST2 data were obtained online at <ftp://ftp.ncdc.noaa.gov/pub/data/ersst-v2>. Analysis has also been performed for monthly mean SST on  $1^\circ \times 1^\circ$  grids from the Hadley Center (HadISST1) for the period 1870–2006 (Rayner et al. 2003). The results from the two SST datasets are quite similar; thus only those based on the ERSST2 are presented.

### 3. Comparison of PDSI and SPI

As both PDSI and SPI are used in measuring droughts, it would be necessary to know how they are related. Some previous studies have compared the behavior of the PDSI and SPI (Guttman 1998; Heim 2002; Mo and Schemm 2008). The SPI shows the highest correlation with the PDSI at time scales from 6 to 12 months, typically with a maximum correlation around 9 months (Redmond 2002). A cross-spectral analysis between the PDSI and SPI indicates that the 12-month SPI oscillations are most nearly in phase with those in the PDSI (Guttman 1998).

Figure 1 shows the local simultaneous correlation between the PDSI and SPI for June–August (JJA). For SPI at time scales of 1–3 months, the correlation over the conterminous United States is higher in the east than in the west (Figs. 1a–c). The lowest correlation is seen in the Southwest where the correlation coefficient can be below 0.4. For SPI at time scales of 9 months and longer, the higher correlation appears in the middle and western United States except for along the coast in the west (Figs. 1d–g). In general, the PDSI has a higher correlation with short-term SPI in the east and with long-term SPI in the west. One exception is along the northwest coast where the short-term SPI has a higher correlation with the PDSI than does the long-term SPI. The correlation indicates that the PDSI in the west is more closely related to a long-term deficit of precipitation.

### 4. Correlation with the Great Plains drought indices

We start with a correlation analysis of the Great Plains droughts that are often the focus of previous studies (Ting

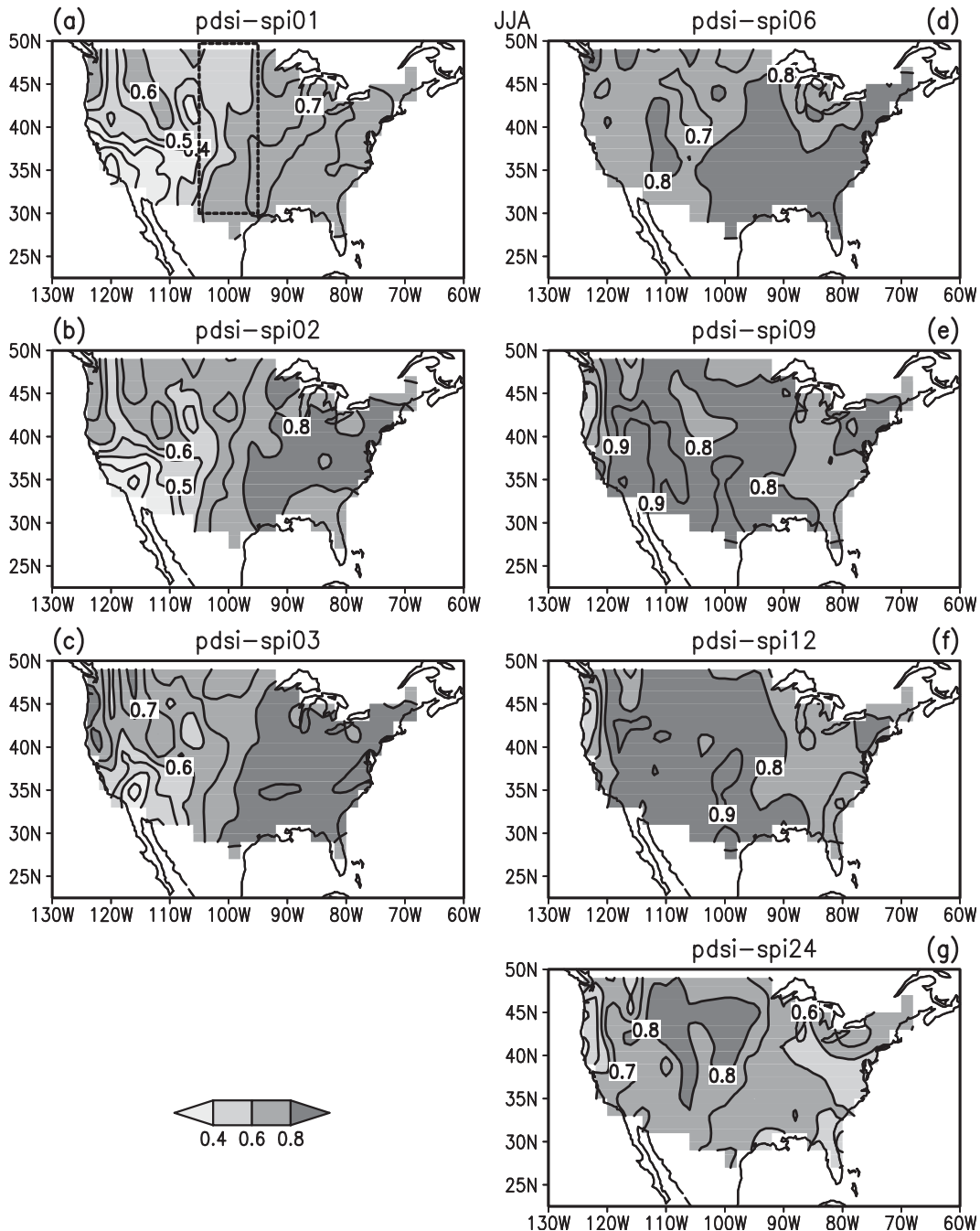


FIG. 1. Local correlation of JJA mean PDSI and SPI during 1897–2007: contour interval is 0.1. The correlation coefficient at the 1% significance level is about 0.25 (or 0.35 for SPI24). The statistical significance is assessed by assuming one degree of freedom per year (or per two years for SPI24) (the same for the other figures). The box in (a) refers to the Great Plains region ( $30^{\circ}$ – $50^{\circ}$ N,  $95^{\circ}$ – $105^{\circ}$ W).

and Wang 1997; Schubert et al. 2004a,b; Seager et al. 2005). Figure 2 shows the correlation of the JJA drought indices in the Great Plains region ( $30^{\circ}$ – $50^{\circ}$ N,  $95^{\circ}$ – $105^{\circ}$ W, the boxed area in Fig. 1a) with global SST in JJA and the preceding December–February (DJF). The Great Plains region is defined as in Schubert et al. (2004b). The SPI03, SPI09, and

SPI24 indices are selected to represent short-, medium-, and long-term droughts, respectively. Note that the correlation maps provide some indication of a cause–effect relationship, but the conclusions should be considered with caution.

The correlation distribution in Fig. 2 broadly resembles the El Niño SST pattern, but with pronounced

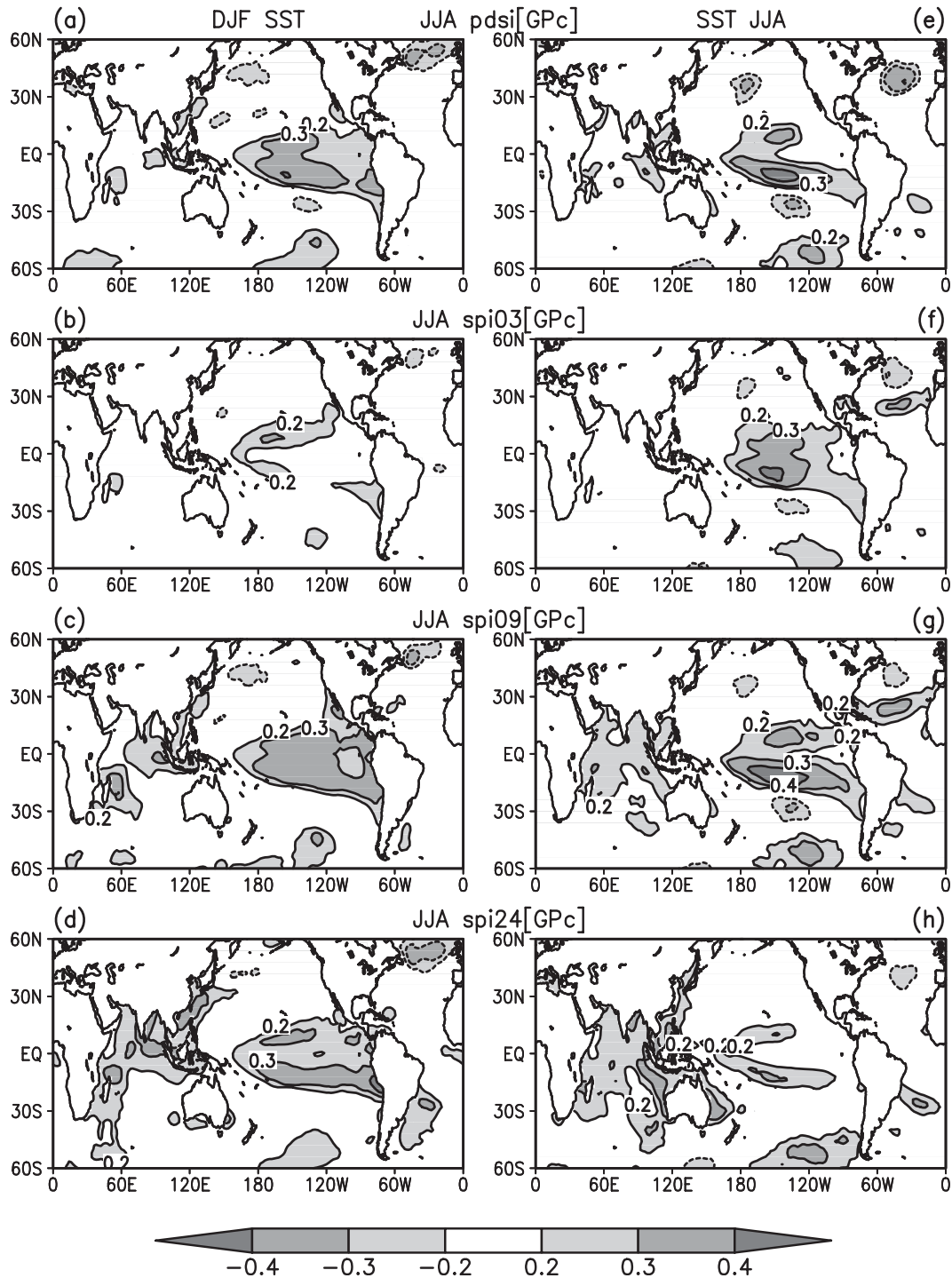


FIG. 2. Correlation of DJF and JJA SST with respect to JJA PDSI and SPI averaged over the Great Plains (30°–50°N, 95°–105°W) during 1897–2005: contour interval is 0.1. Contours with correlation values smaller than 0.2 are suppressed. The correlation coefficient at the 1% significance level is about 0.25 (or 0.35 for SPI24).

differences. There is a region of positive correlation over the central-eastern tropical Pacific and the tropical Indian Ocean, and weak negative correlation extends northeastward and southeastward from the tropical western Pacific. The largest positive correlation tends to be located on the north and south sides of the equatorial Pacific, which differs markedly from the ENSO SST pattern.

Overall, the correlation distribution for PDSI is most similar to that for SPI09. The correlation for SPI03 displays notable differences from that for SPI24, SPI09, and PDSI. The short-term droughts have a better correlation with simultaneous SST than the preceding DJF SST, with noticeable correlation limited to the tropical Pacific Ocean and the North Atlantic Ocean. The medium-term droughts have a good correlation with tropical Pacific SST in both JJA and DJF. The long-term droughts have a better correlation with the tropical Pacific SST in DJF than JJA. SPI09 and SPI24 display a positive correlation with SST in the tropical Indian Ocean in both DJF and JJA. In comparison, the PDSI has a weaker correlation in the tropical Indian Ocean. The positive correlation extends to the South China Sea and the East Asian coastal region. All indices show a negative correlation with DJF SST in the midlatitude North Atlantic Ocean. In the North Atlantic Ocean, the SPI03 and SPI09 have a similar correlation with JJA SST, with positive correlation in the subtropics and negative correlation in the midlatitudes; whereas the correlation for PDSI and SPI24 is only seen in the midlatitudes. There is a negative correlation in the midlatitudes of the North Pacific for PDSI, SPI03, and SPI09 in JJA and for PDSI and SPI09 in DJF, but the area covered is relatively small.

The connection between remote SST forcing and Great Plains droughts could be through soil moisture and surface evaporation variations induced by precipitation anomalies associated with SST-forced large-scale circulation changes over the Pacific–North American region (Namias 1955; Chang and Wallace 1987; Trenberth and Guillemot 1996; Schubert et al. 2004b, 2008; Seager et al. 2005; Seager 2007). Figure 3a shows the simultaneous correlation of SST with DJF precipitation over the Great Plains. From Fig. 3a, cold central-eastern tropical Pacific corresponds to below-normal precipitation over the U.S. Great Plains. Such a relationship has been pointed out in previous studies (e.g., Ropelewski and Halpert 1986; Ting and Wang 1997). Presumably, below-normal precipitation may lead to drier soil moisture after winter. As such, Great Plains soil moisture changes are related to remote SST forcing.

The connection between SST and Great Plains soil moisture and evaporation is confirmed in Figs. 3b–e,

which show the correlation of global SST with Great Plains soil moisture in DJF and March–May (MAM) and evaporation in MAM and JJA derived from the one-layer hydrologic model. The above seasons are shown because the correlation is most significant in these seasons. The soil moisture and evaporation changes in the Great Plains have a significant correlation with SST changes in the tropical Pacific Ocean, tropical Indian Ocean, and midlatitude North Atlantic Ocean. The correlation distributions in Figs. 3b–e are similar to those seen in the correlation of PDSI, SPI09, and SPI24 (Figs. 2a,c,d) and precipitation (Fig. 3a). In comparison, the correlations for soil moisture and evaporation are obviously larger than those in Figs. 2 and 3a. The results support the role of soil moisture changes in connecting the remote SST forcing and summer Great Plains droughts.

Next, we analyze the relationship between drought and soil moisture. We first compare the lag–lead correlation derived from the one-layer hydrological model (Fan and van den Dool 2004) and observations. This is done for the Illinois region where station soil moisture observations are available. Shown in Fig. 4 are correlations for PDSI, SPI03, SPI09, and SPI24 calculated for all months. From Fig. 4, it is clear that the one-layer hydrological model captures the observed drought–soil moisture relationship quite well. The simultaneous correlation coefficient of soil moisture from the one-layer hydrological model and from station observations is close to 0.8. Note that the lag–lead correlation between the model and observed soil moisture (the black curves in Fig. 4) is not symmetric with respect to lag 0. The correlation when the model lags the observations is higher than the corresponding one when the model leads the observations. This discrepancy occurs likely because in the model the soil moisture is precipitation driven.

The soil moisture–drought relationship has a strong dependence on the time scale of droughts. The difference is more prominent when the soil moisture leads. For SPI03, the decrease in the correlation is slower when the soil moisture lags than when the soil moisture leads. This indicates that the impact of precipitation on the soil moisture is likely larger than the impact of soil moisture on precipitation in short-term droughts. For SPI09 and SPI24, the lead correlation is much larger than the lag correlation, suggesting the important role of soil moisture in the development of medium-term and long-term droughts. For PDSI, the correlation is more symmetric, which is similar to SPI06 (not shown).

Figure 5 shows the lead–lag correlation of soil moisture and evaporation with reference to JJA drought indices for the Great Plains region. For SPI03, the soil moisture shows the highest correlation at lag 0, a quick

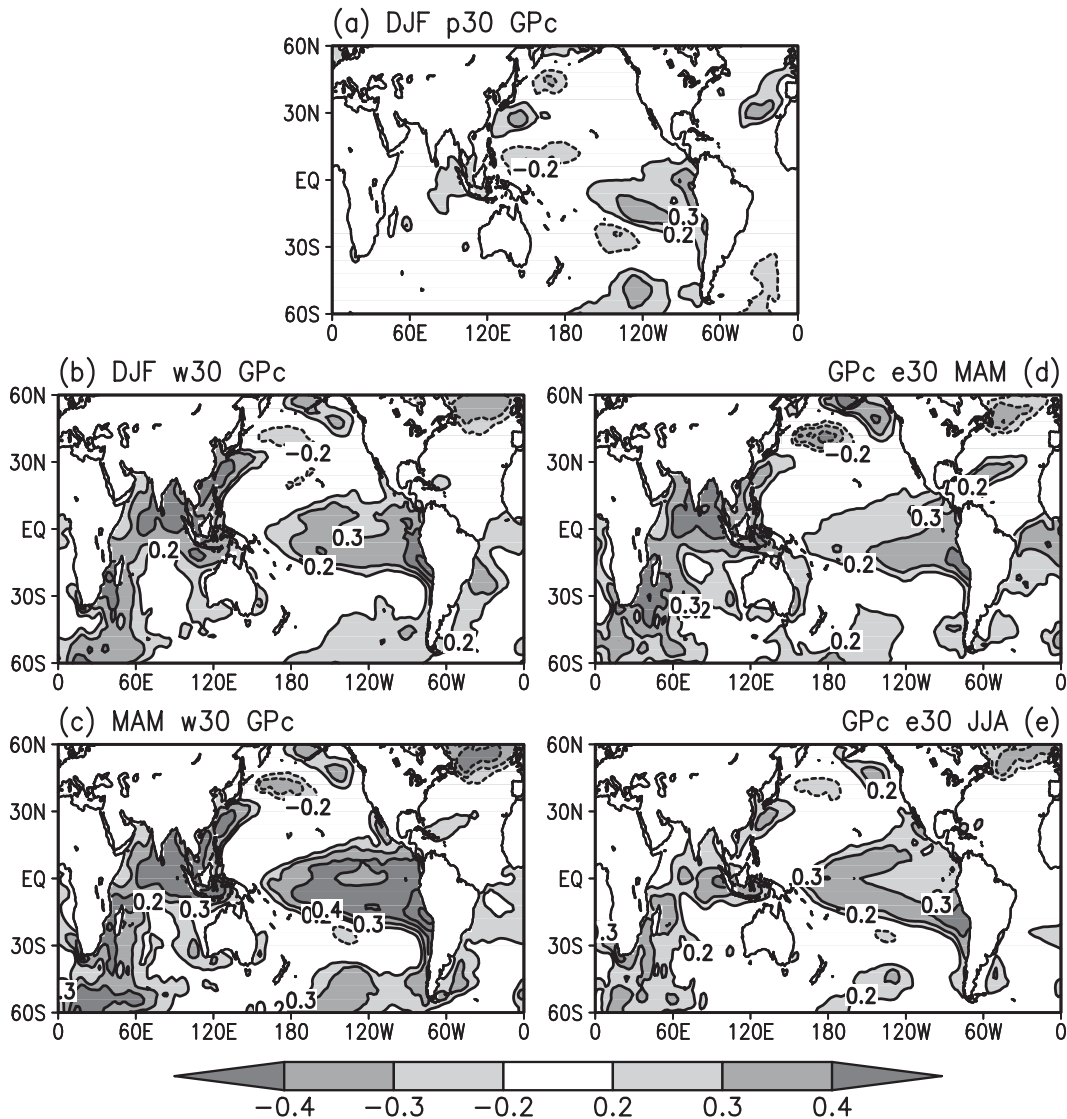


FIG. 3. Correlation of DJF SST with (a) DJF precipitation, (b) DJF and (c) MAM soil moisture, and (d) MAM and (e) JJA evaporation averaged over the Great Plains ( $30^{\circ}$ – $50^{\circ}$ N,  $95^{\circ}$ – $105^{\circ}$ W) during 1932–2005: contour interval is 0.1. Contours with correlation values smaller than 0.2 are suppressed. The correlation coefficient at the 1% significance level is about 0.30.

drop of correlation in the first two lag months, and a period of about six months with a relatively steady correlation (Fig. 5a). The flat curves around +6 month occur because soil moisture changes little in winter when there is snow or frozen ground. The evaporation correlation is largest at lag 0–1 month (Fig. 5b). This indicates a sequence of precipitation, soil moisture, and evaporation changes for short-term droughts. For PDSI, the lag–lead correlation is fairly symmetric. For SPI09, the soil moisture has the largest correlation at 1-month lead. The evaporation correlation tends to be symmetric. Soil moisture and evaporation changes apparently lead SPI24. Note that the evaporation correlation is quite

large in the previous summer but relatively small during November–March, indicating the seasonality of evaporation impacts. In winter, evaporation is small owing to low temperature. In summer, evaporation impacts increase due to the soil moisture control. The large correlation in JJA common to different time scales suggests that the contribution of soil moisture to summer droughts may be through surface evaporation, as suggested by previous studies (Atlas et al. 1993; Lyon and Dole 1995; Trenberth and Guillemot 1996), although the cause–effect relationship needs to be validated. In comparison, the lag–lead correlation suggests that, for short-term droughts, the precipitation impacts are larger than the soil

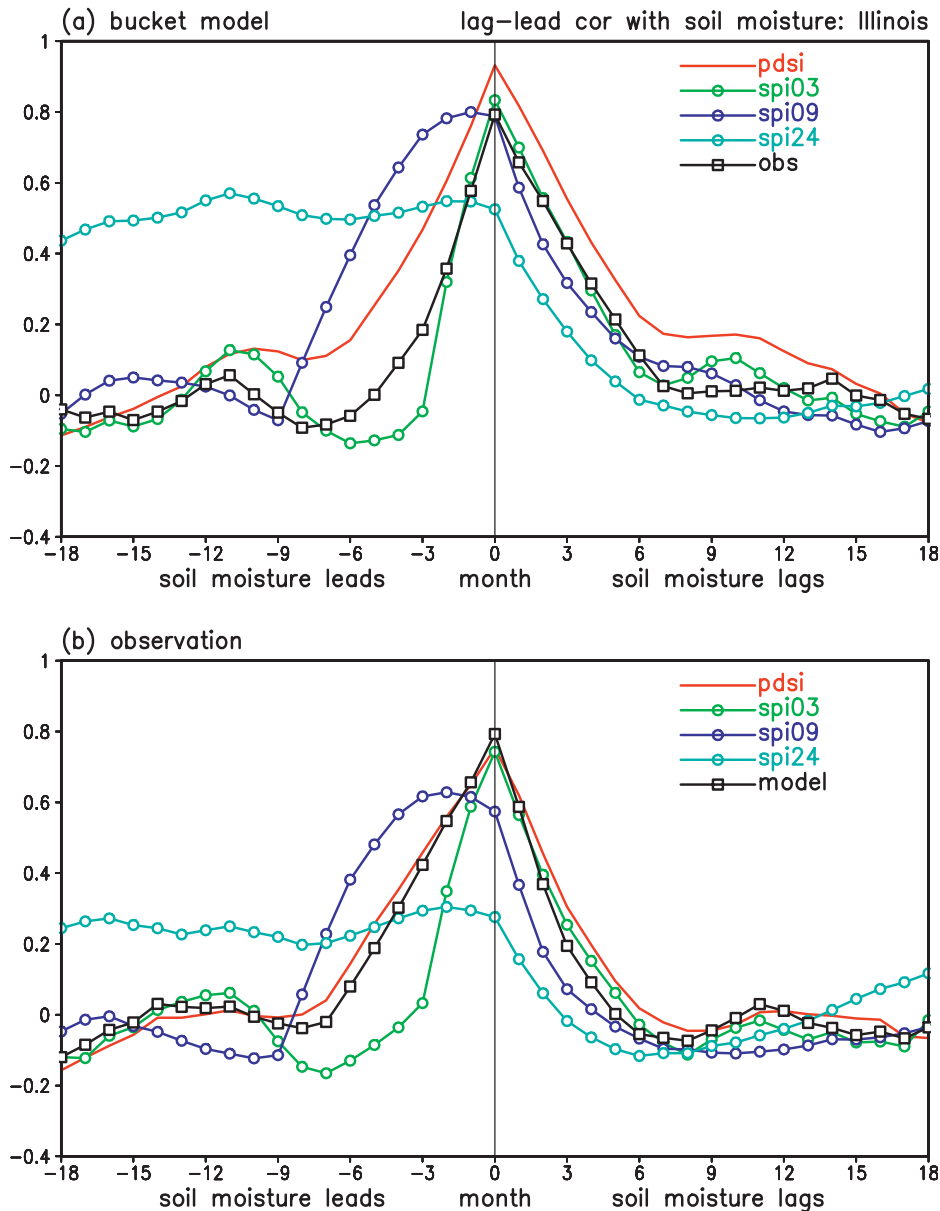


FIG. 4. (a) Lag–lead correlation of soil moisture from the bucket model with respect to PDSI, SPI, and observed soil moisture averaged over Illinois during 1984–2004. (b) Similar to (a), except for soil moisture from observations. The correlation coefficient at the 5% significance level is about 0.44 (or 0.60 for SPI24).

moisture impacts, whereas for medium-term and long-term droughts, the soil moisture impacts are pronounced.

We also examined the lag–lead correlation based on the VIC soil moisture. The evolution of lead–lag correlation (not shown) is very similar to that based on the one-layer hydrologic model soil moisture. The consistency between the two models provides support for the drought–soil moisture relationship described above.

The above correlation analyses are affected by the persistence of soil moisture and the property of the SPI.

The soil moisture anomalies are caused by precipitation anomalies and soil moisture has a much redder spectrum than precipitation. This alone could lead to high correlations of soil moisture with preceding SST. The SPI is defined based on past rainfall, so the asymmetry in correlation seen in Figs. 4 and 5 may be a property of the SPI definition. Here, we validate the roles of soil moisture using Findell and Eltahir’s (1997) method.

There are three possible explanations for the results of correlation analyses. First, persistent external forcing

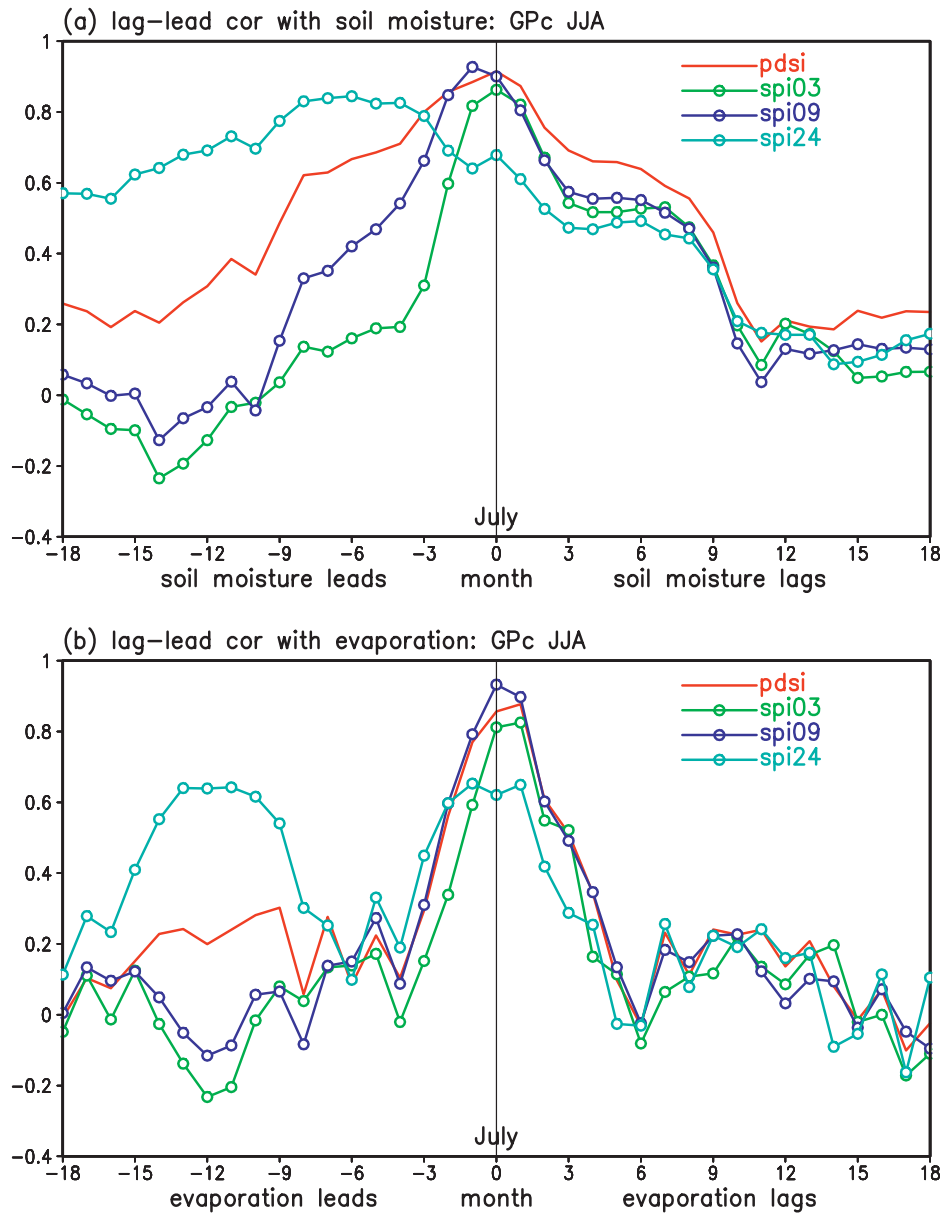


FIG. 5. Lag-lead correlation of (a) soil moisture and (b) evaporation with respect to PDSI and SPI averaged over the Great Plains (30°–50°N, 95°–105°W) during 1932–2005. The correlation coefficient at the 1% significance level is about 0.30 (or 0.40 for SPI24).

(e.g., SST) sustains the persistence of drought from winter to summer. The persistence is also partly due to the intrinsic property of the medium- and long-term SPIs. Through the correlation between concurrent rainfall and soil moisture in winter–spring, a correlation appears between the winter–spring soil moisture and the summer SPI. Second, the persistence of the drought is due to the positive feedback of soil moisture. Precipitation anomalies in winter initiate soil moisture anomalies in winter–spring that, in turn, favor the maintenance of the

precipitation anomalies in the subsequent summer. Third, the above two mechanisms combine to contribute to the persistence of drought from winter to summer. According to Findell and Eltahir (1997), in the first case, it would be expected that the autocorrelation of SPI from winter to summer would be greater than the correlation between the winter–spring soil moisture and the summer SPI whereas, in the second case, the opposite would be expected.

Table 1 shows the autocorrelation of drought indices between winter and summer and the correlation between

TABLE 1. Autocorrelations of drought indices from winter to summer and correlations between the winter or spring soil moisture and the summer drought indices for the Great Plains during 1932–2005.

	Autocorrelation	Soil (DJF)–drought (JJA)	Soil (MAM)–drought (JJA)
PDSI	0.71	0.67	0.85
SPI01	0.27	0.27	0.37
SPI02	0.28	0.26	0.42
SPI03	0.26	0.21	0.44
SPI06	0.26	0.25	0.61
SPI09	0.31	0.44	0.74
SPI12	0.51	0.71	0.86
SPI24	0.83	0.85	0.84

the winter or spring soil moisture and the summer drought indices. From this table, the correlation between the summer drought indices and the winter soil moisture are comparable to the corresponding autocorrelation of drought indices, except for SPO09 and SPI12 for which the soil moisture correlation is larger than the autocorrelation of SPI. The summer drought indices are better correlated with the spring soil moisture than with the winter drought indices except for SPI24. This suggests that the soil moisture feedback likely contributes more to the persistence of drought from winter to summer. This, however, cannot rule out the possibility that the external forcing also makes a contribution. A higher correlation of MAM soil moisture than DJF soil moisture may be due to snowpack. DJF soil moisture in the Great Plains may be quite constant as a consequence of the effect of snowpack. During the snow-melting season (MAM), the amount of snowpack laid down in the preceding winter may be important to explain the soil moisture. Hence, the MAM soil moisture may be more highly correlated with droughts at long time scales. Again, the soil moisture itself is related to SST-forced precipitation in winter.

The correlation in Table 1 is higher for medium-term and long-term droughts than for short-term droughts. This may be related to the inherent time scales in drought indices. For SPI longer than 6 months, the winter precipitation is involved in the calculation of the SPI indices for summer. At the same time, winter precipitation also contributes to soil moisture in winter and spring, which would lead to a correlation between winter–spring soil moisture and summer droughts at medium and long time scales.

### 5. Correlation with the Niño-3.4 SST

Previous studies have emphasized the role of ENSO in U.S. climate. Here, we conduct a correlation analysis with the Niño-3.4 SST as reference. Figure 6 shows the

correlation of JJA drought indices with respect to DJF and JJA Niño-3.4 ( $5^{\circ}\text{S}$ – $5^{\circ}\text{N}$ ,  $170^{\circ}$ – $120^{\circ}\text{W}$ ) SST.

Figure 6 shows important differences between short-term and long-term droughts. The SPI03 has a higher correlation with JJA Niño-3.4 SST than with DJF Niño-3.4 SST, whereas the PDSI, SPI09, and SPI24 have a larger correlation with DJF than JJA Niño-3.4 SST. Notably, the JJA correlation is large for SPI03 in the Great Plains. The highest DJF correlation for PDSI, SPI09, and SPI24 is found in the Southwest with northward extension into the Great Plains. The correlation distribution for PDSI is consistent with Piechota and Dracup (1996), Cole and Cook (1998), and Rajagopalan et al. (2000). Cole and Cook showed that the correlation in the Great Plains for PDSI appears as an extension from the Southwest. The magnitude of correlation is close for PDSI and SPI09, while the correlation for SPI24 is smaller.

The ENSO impacts on drought could be through soil moisture and evaporation changes induced by precipitation anomalies due to ENSO-forced circulation changes. The influence of ENSO on U.S. precipitation has been shown in previous studies (Ropelewski and Halpert 1986; Piechota and Dracup 1996). Figure 7a shows the simultaneous correlation of Niño-3.4 SST with contiguous U.S. precipitation in DJF. During El Niño years, above-normal precipitation is observed over the southern United States with northward extensions into the Great Plains. The correlation coefficient between DJF Niño-3.4 SST and DJF precipitation in the Great Plains and Southwest during the period 1932–2005 is 0.23 and 0.36, respectively (Table 2). The ENSO-induced precipitation anomalies can, in turn, lead to changes in soil moisture. The correlation coefficient between DJF precipitation and DJF and MAM soil moisture is 0.40 and 0.46 for the Great Plains and 0.61 and 0.71 for the Southwest region ( $30^{\circ}$ – $40^{\circ}\text{N}$ ,  $95^{\circ}$ – $115^{\circ}\text{W}$ ; the boxed area in Fig. 6a), respectively (Table 2). The correlation coefficient between DJF precipitation and MAM and JJA evaporation is 0.47 and 0.31 for the Great Plains and 0.67 and 0.60 for the Southwest, respectively (Table 2). These

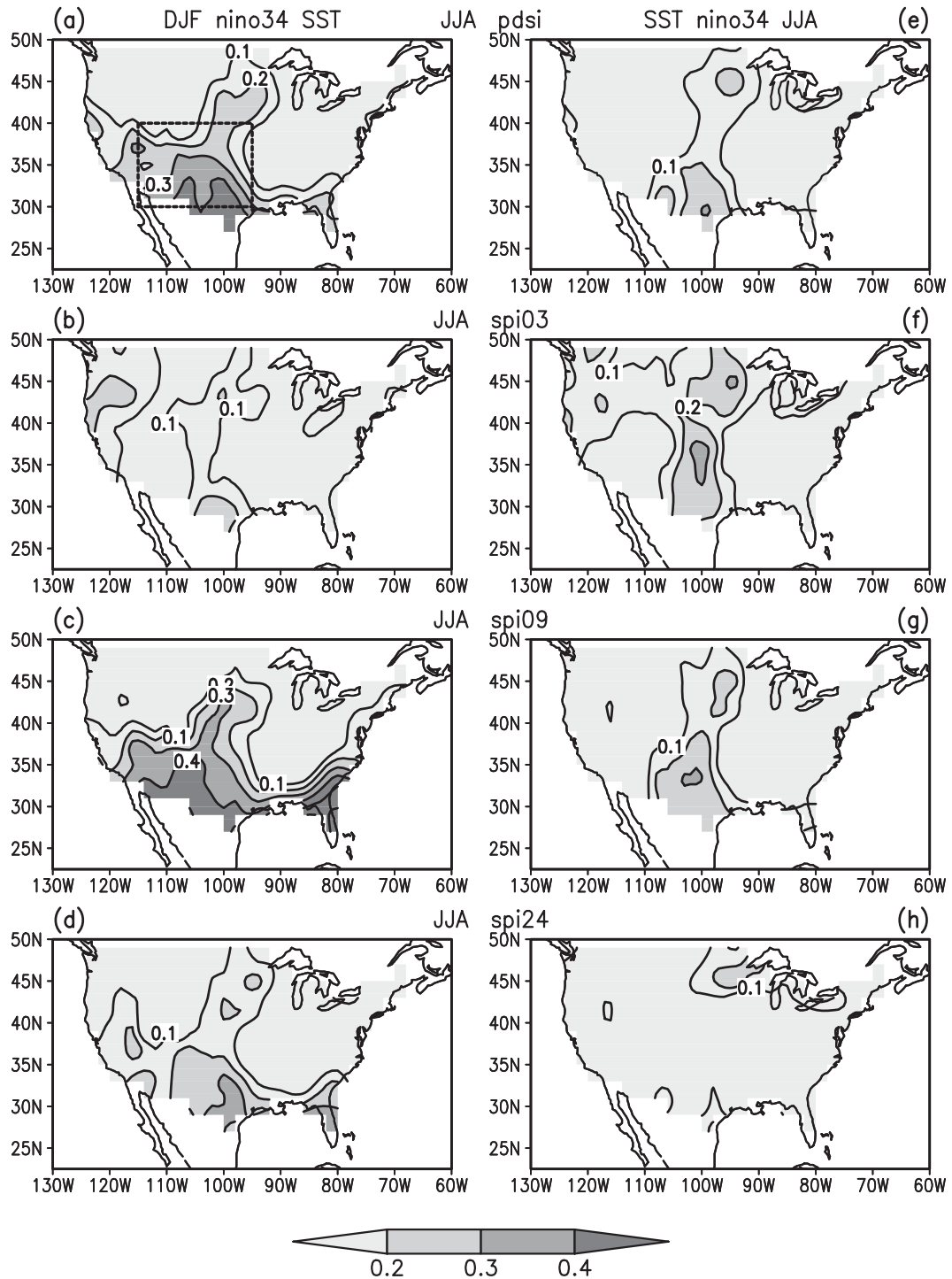


FIG. 6. Correlation of JJA PDSI and SPI with respect to DJF and JJA Niño-3.4 SST during 1897–2005. The contour interval is 0.1. The correlation coefficient at the 1% significance level is about 0.25 (or 0.35 for SPI24). (a) The box refers to the Southwest (30°–40°N, 95°–115°W).

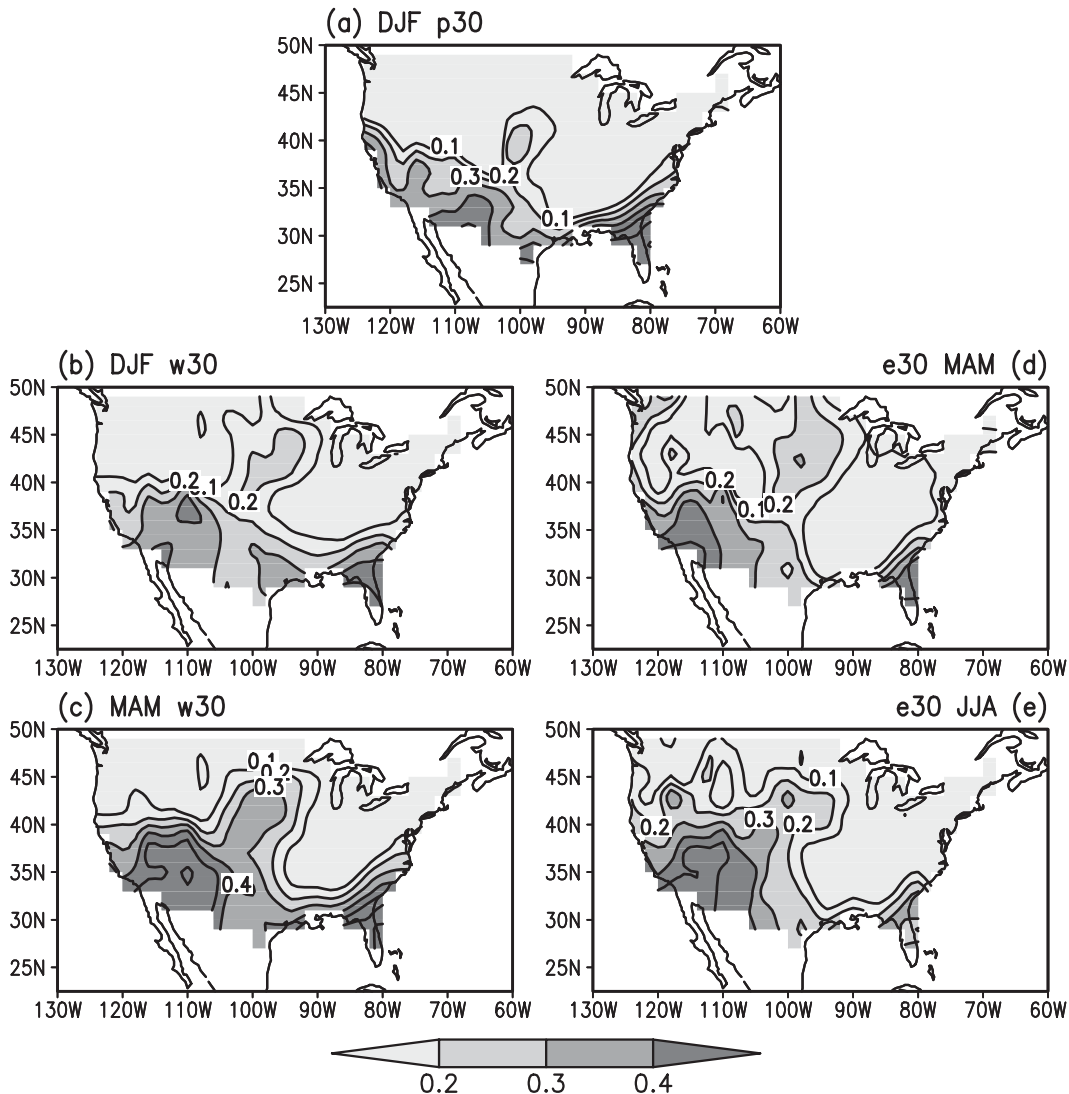


FIG. 7. Correlation of (a) DJF precipitation, (b) DJF and (c) MAM soil moisture, and (d) MAM and (e) JJA evaporation with respect to DJF Niño-3.4 SST during 1932–2005; contour interval is 0.1. The correlation coefficient at the 1% significance level is about 0.30.

correlations suggest that ENSO can induce soil moisture changes in the contiguous United States.

The connection between ENSO and U.S. soil moisture is confirmed by Figs. 7b–e, which show the correlation of DJF and MAM soil moisture and MAM and JJA surface evaporation with respect to DJF Niño-3.4 SST. Obviously, the correlation distribution is similar to that in Fig. 7a. The correlation distribution also resembles closely that seen in Figs. 6a,c,d, but with a larger magnitude. The largest correlation is seen in the Southwest with extensions into the Great Plains. This supports earlier findings that the most pronounced hydrologic impacts of ENSO are in the southwestern United States.

The ENSO impacts are further demonstrated by the lead–lag correlation of the drought indices averaged over the Southwest with respect to DJF Niño-3.4 SST, shown in Fig. 8. In general, the correlation coefficients in Fig. 8 are not high. Significant correlations are seen during winter through early summer. The ENSO impacts on PDSI, SPI09, and soil moisture are apparent in DJF. The largest correlation is seen in MAM, lagging the ENSO mature phase by about one season. The induced droughts can persist into spring and summer. This persistence seems to be related to the enhanced evaporation in late spring and summer following the increase in soil moisture. This soil moisture–evaporation effect seems especially important for long-term drought that

TABLE 2. Correlation of Niño-3.4 SST in DJF, Great Plains (GP) or Southwest (SW) soil moisture, and evaporation in DJF, MAM, and JJA with respect to GP or SW precipitation in DJF during 1932–2005.

	Niño-3.4 SST		Soil moisture		Evaporation	
	GP	SW	GP	SW	GP	SW
DJF	0.23	0.36	0.40	0.61	0.16	0.20
MAM			0.46	0.71	0.47	0.67
JJA			0.34	0.55	0.31	0.60

develops after DJF. Note that the evaporation correlation is small in DJF and becomes large in late spring and summer, indicating a delayed feedback of soil moisture on droughts through evaporation, which may be related to the annual cycle of insolation and temperature. There is a similar feature in the Great Plains region except that the correlation is weaker (not shown). The lag–lead correlation was also calculated for a smaller domain ( $30^{\circ}$ – $35^{\circ}$ N,  $95^{\circ}$ – $105^{\circ}$ W). The results are similar except the correlation is somewhat weaker (figures not shown).

The positive correlation with JJA SST in the subtropical North Atlantic Ocean for SPI03 and SPI09 (Fig. 2) suggests a possible impact of the North Atlantic SST. This is confirmed by a correlation analysis with the subtropical North Atlantic JJA SST as a reference. The results (figures not shown) indicate that the subtropical North Atlantic JJA SST contributes to the Great Plains droughts but is secondary to the effect of tropical Pacific SST. For PDSI and SPI24, the notable correlation is

limited to southern Great Plains. For SPI03 and SPI09, the impacts extend to the northern Great Plains.

## 6. Long-term changes in the SST–drought correlation

The correlation presented in previous sections is calculated based on the whole period. One question is whether the SST–drought relationship has changed with time during the analysis period. There is an indication of long-term changes in the relationship between U.S. drought and SST forcing (Cole and Cook 1998; Rajagopalan et al. 2000). Such changes may indicate strengthening or weakening of SST forcing for droughts. It is important to reveal such changes for a better understanding of the role of SST forcing for droughts.

To examine the long-term changes in the SST–drought relationship with time, we show in Fig. 9 the sliding correlation between Niño-3.4 SST and drought indices using a 31-yr window. A similar sliding correlation for the tropical Indian Ocean (TIO) SST ( $15^{\circ}$ S– $15^{\circ}$ N,  $50^{\circ}$ – $100^{\circ}$ E) is shown in Fig. 10. In these figures, drought indices in both the Great Plains and U. S. Southwest are considered.

The DJF Niño-3.4 SST shows a robust positive correlation with PDSI, SPI09, and SPI24 in the Southwest during the whole period, but the magnitude of correlation varies largely (Fig. 9a). The correlation of SPI03 in the Southwest with DJF Niño-3.4 SST displays an apparent contrast before and after the mid-1950s. For

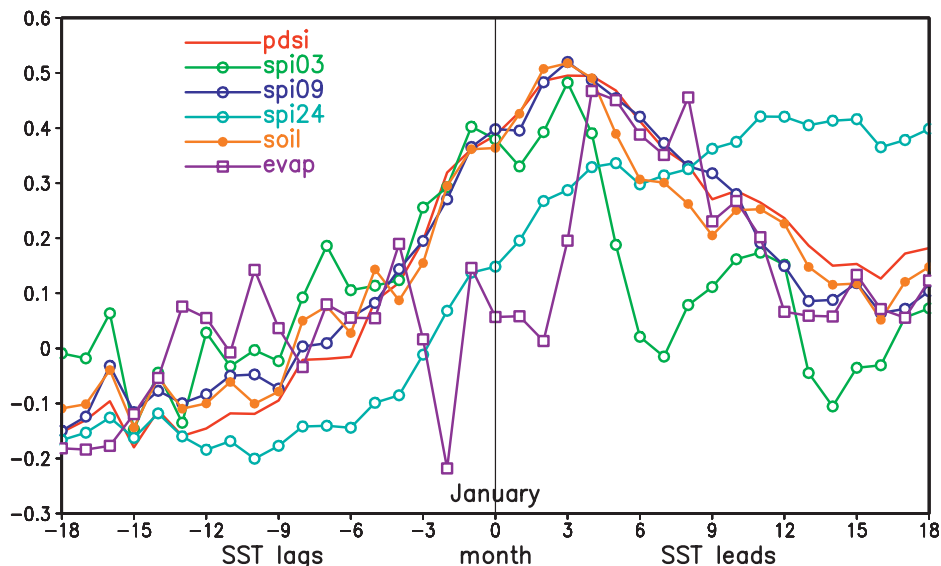


FIG. 8. Lag–lead correlation of the Southwest ( $30^{\circ}$ – $40^{\circ}$ N,  $95^{\circ}$ – $115^{\circ}$ W) PDSI, SPI, soil moisture, and evaporation with respect to DJF Niño-3.4 SST during 1932–2005. The correlation coefficient at the 1% significance level is about 0.30 (or 0.40 for SPI24).

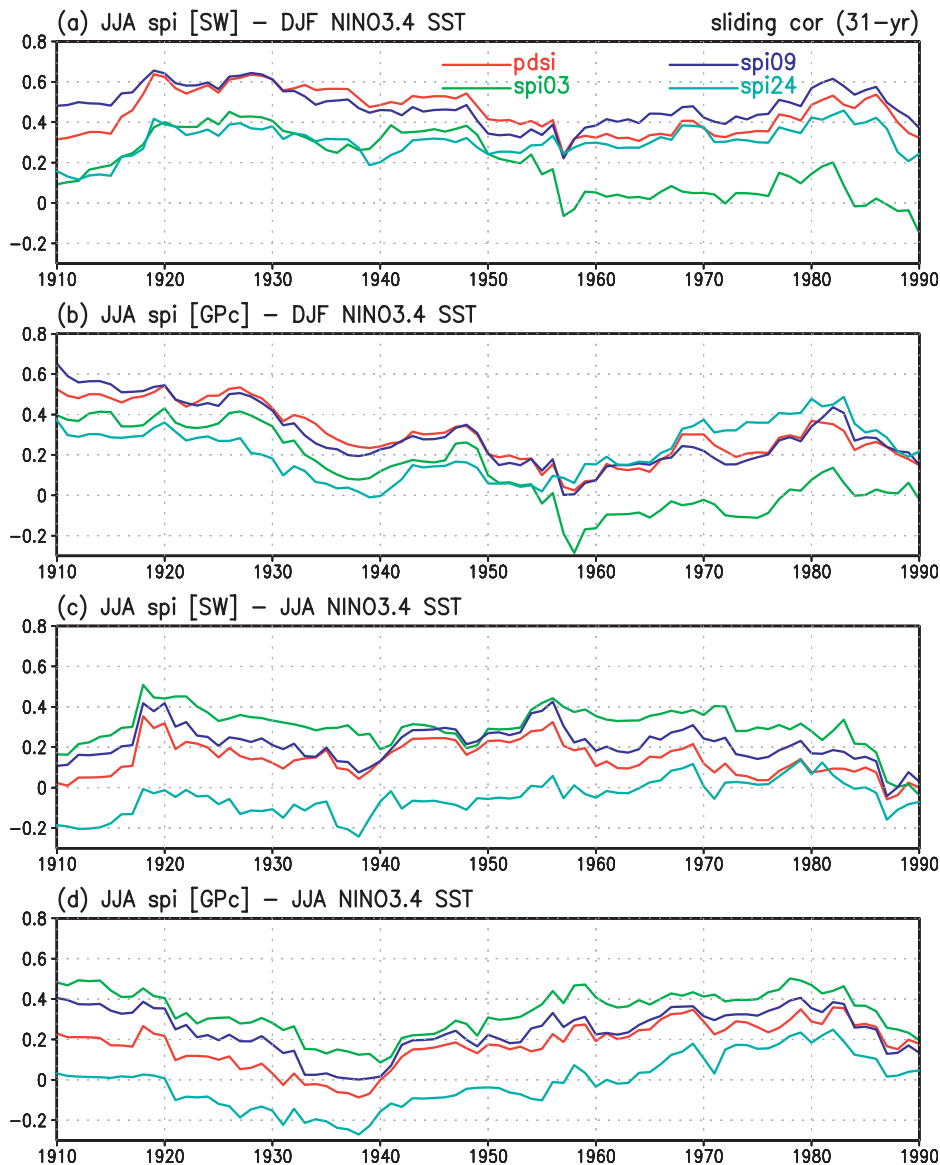


FIG. 9. Sliding correlation between DJF or JJA Niño-3.4 SST and JJA Southwest or Great Plains PDSI and SPI with a 31-yr window. The correlation shown in the figure is for the center year of the window. The correlation coefficient at the 5% significance level is about 0.36 (or 0.50 for SPI24).

the Great Plains region, the correlation with the DJF Niño-3.4 SST shows an overall weakening with time until the mid-1950s (Fig. 9b). After that, the correlation tends to increase until the early 1980s, which is then followed by a weakening in the correlation. In comparison, the correlation change is relatively smaller for the Southwest than for the Great Plains. Note that, after the mid-1950s, the correlation for SPI03 is weaker than that for PDSI, SPI09, and SPI24 for both the Southwest and the Great Plains, consistent with Figs. 2 and 6.

The JJA Niño-3.4 SST has a higher correlation with SPI03 than with PDSI, SPI09, and SPI24 for both the

Southwest and the Great Plains (Figs. 9c,d), which is consistent with Figs. 2 and 6. In comparison, the correlation change is relatively smaller for the Southwest than for the Great Plains, which is similar for DJF. For the Great Plains, the correlation decreases in the early period until the late 1930s (Fig. 9d). After that, the correlation increases until the early 1980s, which is then followed by a weakening in the correlation.

The DJF TIO SST shows a relatively steady positive correlation with PDSI, SPI09, and SPI24 in the Southwest before the mid-1980s (Fig. 10a). The correlation, however, has dropped quickly since then. The correlation for

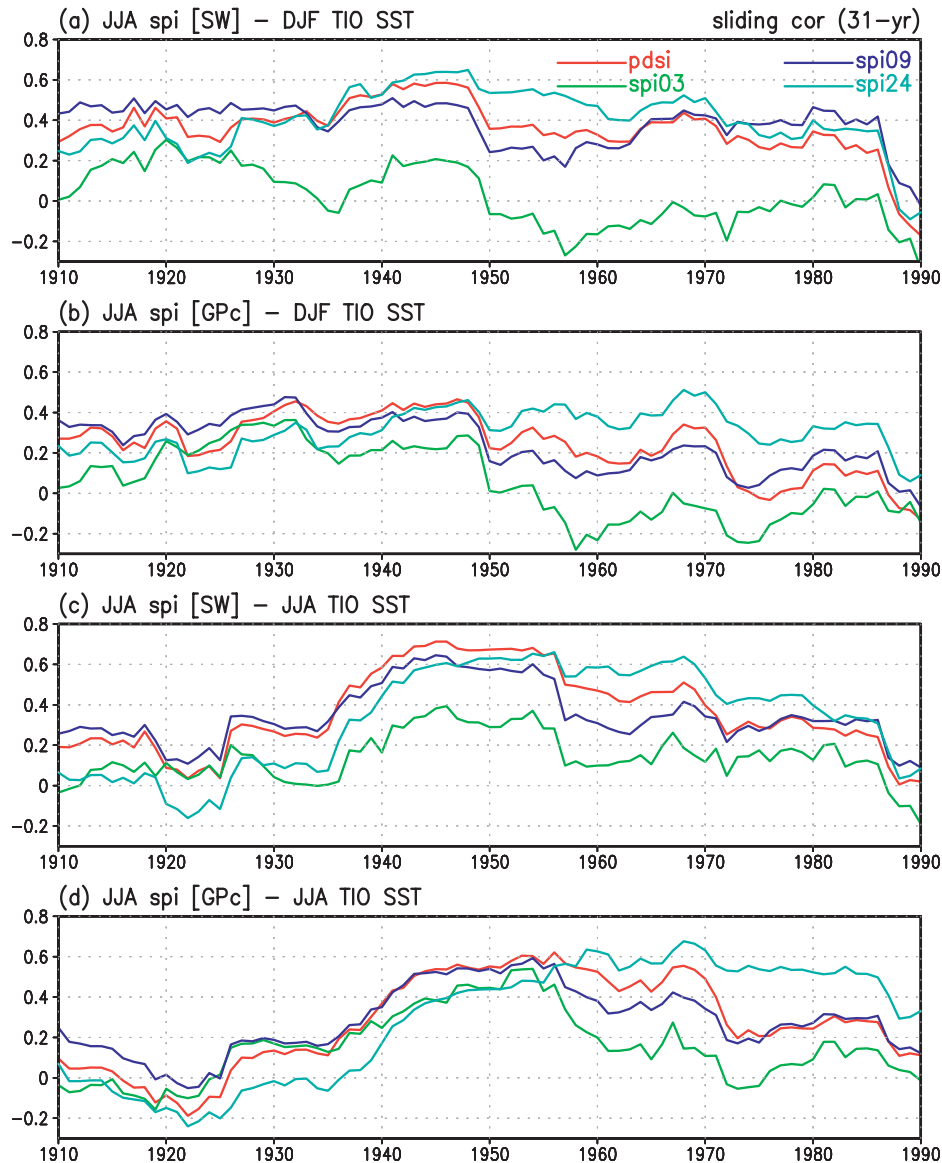


FIG. 10. As in Fig. 9, but for the tropical Indian Ocean ( $15^{\circ}\text{S}$ – $15^{\circ}\text{N}$ ,  $50^{\circ}$ – $100^{\circ}\text{E}$ ) SST.

SPI03 is generally weak during the period. The correlation for the Great Plains displays long-term changes with time (Fig. 10b) similar to those in the Southwest. The correlation for the SPI03 shows an obvious transition from positive to negative around 1950, a feature seen in both the Southwest and the Great Plains (Figs. 10a,b).

The JJA TIO SST correlation shows a more pronounced change with time compared to the DJF TIO SST. Before the late 1930s, the correlation is generally weak for both the Southwest and Great Plains (Figs. 10c,d). The correlation underwent an obvious increase from the late 1930s to the mid-1940s. After a relatively steady period of about 10 years, the correlation displays an overall decrease with time for PDSI, SPI09, and

SPI24 in the Southwest, and for PDSI and SPI09 in the Great Plains. The SPI24 in the Great Plains maintained a steady positive correlation from the 1960s to the mid-1980s (Fig. 10d).

One issue is whether the long-term changes in the SST–drought correlation are significantly larger than might be expected from noise effects. Gershunov et al. (2001) performed bootstrapped tests and constructed a table (their Table 1) that gives the 95% percentile of the bootstrapped standard deviation corresponding to a specific mean correlation. The standard deviation of sliding correlations between two time series must be outside those limits to be considered significantly more variable than expected from noise.

We calculated the means and standard deviations of the sliding correlations and compared these with Table 1 of Gershunov et al. (2001). It turns out that most of the correlations in Figs. 9 and 10 are within the range of fluctuations due to noise effects. This suggests that stochastic processes may play a role in the correlation changes. However, there are three curves whose standard deviations are above the 95% percentile of the bootstrapped standard deviation. All of these three curves are correlations with the JJA TIO SST. One is the PDSI in the Great Plains (Fig. 10d); the other two are the SPI24 in both the Great Plains and Southwest (Figs. 10c,d).

In summary, the relationship between ENSO and medium-term and long-term droughts over the Southwest is relatively steady during the analysis period although there are some variations in the intensity of the relationship. The relationship for the Great Plains droughts has experienced large changes during the analysis period: strong in the early period, quite weak in the 1950s and 1960s, and strong in the 1970s and 1980s. Our results are consistent with Cole and Cook (1998). For Great Plains summer droughts, the long-term changes in the relationship with Niño-3.4 SST differ between DJF and JJA SST. Another important finding is the pronounced changes in the relationship of summer droughts with simultaneous tropical Indian Ocean SST, especially for long-term droughts. This suggests that the impacts of the tropical Indian Ocean on U.S. summer droughts may have increased in the second half of the twentieth century.

## 7. Summary

Based on the SPI indices, the present study distinguishes droughts at different time scales. It is found that the relationship between SST and soil moisture and boreal summer U.S. droughts differs significantly between short-term and long-term droughts. The main results are as follows:

- Short-term Great Plains droughts have a good correlation only with simultaneous SST in the tropical Pacific and subtropical North Atlantic Ocean, with cold SST in the above regions corresponding to droughts. Medium-term and long-term Great Plains droughts have a good correlation with both simultaneous and preceding SST in the tropical Pacific and Indian Oceans. The medium-term droughts have a good correlation with simultaneous SST in the subtropical North Atlantic.
- The Great Plains soil moisture in winter–spring and surface evaporation in spring–summer have a good correlation with winter SST in many regions, including the tropical Pacific and Indian Oceans.

- For short-term droughts, the drought–soil moisture correlation tends to be contemporaneous. For medium-term and long-term droughts, the soil moisture changes lead the droughts.
- The highest correlation of U.S. droughts, as well as soil moisture and surface evaporation, with preceding eastern equatorial Pacific SST is in the Southwest with extensions into the Great Plains.
- The relationship between tropical Pacific Ocean SST and boreal summer U.S. droughts has undergone obvious long-term changes. The long-term change is more pronounced for Great Plains droughts than for Southwest droughts. Long-term changes are also apparent in the correlation of U.S. droughts with tropical Indian Ocean SST, especially for JJA SST.

The above results indicate that the short-term droughts are mostly influenced by simultaneous remote SST forcing, and the medium-term and long-term droughts are influenced by both preceding and simultaneous remote SST forcing. The anomalous soil moisture can contribute to the persistence of droughts through a positive soil moisture–precipitation feedback. The most important remote forcing for U.S. summer droughts is from the tropical Pacific SST. For medium-term and long-term droughts, tropical Indian Ocean SST forcing also contributes to droughts. Additional impacts for short-term and medium-term droughts are related to the North Atlantic SST forcing. The most notable impacts of the tropical Pacific SST forcing on medium-term and long-term droughts are found in the Southwest with extensions into the Great Plains.

The antecedent SST forcing affects the summer droughts through soil moisture and evaporation changes. The processes may be as follows. SST forcing induces atmospheric circulation and precipitation anomalies. The precipitation changes affect winter–spring soil moisture and the spring–summer surface evaporation. The induced soil moisture and surface evaporation anomalies then contribute to summer droughts.

Most previous studies on U.S. droughts do not explicitly separate the time scales of droughts. Some studies focus on long-term droughts by low-pass filtering (e.g., Schubert et al. 2004a,b; Seager et al. 2005; Mo and Schemm 2008). A unique feature of the present study is separating and comparing the relationship for droughts at different time scales utilizing the SPI. The results suggest that the roles of SST and soil moisture for summer droughts depend critically on the time scales. Thus, it would be necessary to distinguish the time scales of droughts in future studies for a better understanding of the causes of the droughts and roles of SST forcing and soil moisture feedbacks to droughts.

The present study is mainly a correlation analysis. Thus, the results on the roles of SST forcing and soil moisture in U.S. summer droughts should be considered with caution. Further studies will be needed to demonstrate the cause–effect relationship, including carefully designed numerical experiments for this purpose.

The identified long-term changes in the SST–drought index correlation suggest that the impacts of tropical Indo-Pacific SST on U.S. summer droughts are not stationary. The reasons for the long-term changes in the SST–drought relationship need to be investigated in the future. Plausible reasons may include changes in the mean state (Cole and Cook 1998; White et al. 2008) and SST variance (Cole and Cook 1998) and interdecadal modes (Cole and Cook 1998; Hu and Huang 2007). For example, is the increase in the tropical Indian Ocean SST–U.S. drought correlation related to the tropical Indian Ocean warming? Understanding reasons for long-term changes has important implications for applications of the relationship to forecasts of droughts.

*Acknowledgments.* Comments of Paul Dirmeyer and two anonymous reviewers have led to a significant improvement of the manuscript. This research was supported by grants from the NSF (ATM-0332910), NOAA (NA04OAR4310034 and NA05OAR4311135), and NASA (NNG04GG46G).

#### REFERENCES

- Alexander, M. A., I. Bladé, M. Newman, J. R. Lanzante, N.-C. Lau, and J. D. Scott, 2002: The atmospheric bridge: The influence of ENSO teleconnections on air–sea interaction over the global oceans. *J. Climate*, **15**, 2205–2231.
- Alley, W. M., 1984: The Palmer drought severity index: Limitations and assumptions. *J. Climate Appl. Meteor.*, **23**, 1100–1109.
- Andreadis, K. M., E. A. Clark, A. W. Wood, A. F. Hamlet, and D. P. Lettenmaier, 2005: Twentieth-century drought in the conterminous United States. *J. Hydrometeor.*, **6**, 985–1001.
- Atlas, R., N. Wolfson, and J. Terry, 1993: The effect of SST and soil moisture anomalies on the GLA model simulations of the 1988 U.S. drought. *J. Climate*, **6**, 2034–2048.
- Barlow, M., S. Nigam, and E. H. Berbery, 2001: ENSO, Pacific decadal variability, and U.S. summertime precipitation, drought, and stream flow. *J. Climate*, **14**, 2105–2128.
- Chang, F.-C., and J. M. Wallace, 1987: Meteorological conditions during heat waves and droughts in the United States Great Plains. *Mon. Wea. Rev.*, **115**, 1253–1269.
- Cole, J., and E. Cook, 1998: The changing relationship between ENSO variability and moisture balance in the continental United States. *Geophys. Res. Lett.*, **25**, 4529–4532.
- Conil, S., H. Douville, and S. Tyteca, 2007: The relative influence of soil moisture and SST in climate predictability explored within ensembles of AMIP type experiments. *Climate Dyn.*, **28**, 125–145.
- Dai, A., K. E. Trenberth, and T. R. Karl, 1998: Global variations in droughts and wet spells, 1900–1995. *Geophys. Res. Lett.*, **25**, 3367–3370.
- Dirmeyer, P. A., M. J. Fennessy, and L. Marx, 2003: Low skill in dynamical prediction of boreal summer climate: Grounds for looking beyond sea surface temperature. *J. Climate*, **16**, 995–1002.
- Eltahir, E. A. B., 1998: A soil moisture-rainfall feedback mechanism. 1: Theory and observations. *Water Resour. Res.*, **34**, 765–776.
- Fan, Y., and H. M. van den Dool, 2004: Climate Prediction Center global monthly soil moisture data set at 0.5° resolution for 1948 to present. *J. Geophys. Res.*, **109**, D10102, doi:10.1029/2003JD004345.
- Fennessy, M. J., and J. Shukla, 1999: Impact of initial soil wetness on seasonal atmospheric prediction. *J. Climate*, **12**, 3167–3180.
- Findell, K. L., and E. A. B. Eltahir, 1997: An analysis of the soil moisture-rainfall feedback, based on direct observations from Illinois. *Water Resour. Res.*, **33**, 725–735.
- Gershunov, A., N. Schneider, and T. P. Barnett, 2001: Low-frequency modulation of the ENSO–Indian monsoon rainfall relationship: Signal or noise? *J. Climate*, **14**, 2486–2492.
- Giorgi, F., L. O. Mearns, C. Shields, and L. Mayer, 1996: A regional model study of the importance of local versus remote controls of the 1988 drought and 1993 flood over the central United States. *J. Climate*, **9**, 1150–1162.
- Guttman, N. B., 1998: Comparing the Palmer drought index and the standardized precipitation index. *J. Amer. Water Resour. Assoc.*, **34**, 113–121.
- , 1999: Accepting the standardized precipitation index: A calculation algorithm. *J. Amer. Water Resour. Assoc.*, **35**, 311–322.
- , J. R. Wallis, and J. R. M. Hosking, 1992: Spatial comparability of the Palmer drought severity index. *Water Resour. Bull.*, **28**, 1111–1119.
- Hayes, M. J., M. D. Svoboda, D. A. Wilhite, and O. V. Vanyarkho, 1999: Monitoring the 1996 drought using the standardized precipitation index. *Bull. Amer. Meteor. Soc.*, **80**, 429–438.
- Heim, R. R., Jr., 2002: A review of twentieth-century drought indices used in the United States. *Bull. Amer. Meteor. Soc.*, **83**, 1149–1165.
- Hoerling, M., and A. Kumar, 2003: The perfect ocean for drought. *Science*, **299**, 691–694.
- Hollinger, S. E., and S. A. Isard, 1994: A soil moisture climatology of Illinois. *J. Climate*, **7**, 822–833.
- Hong, S.-Y., and E. Kalnay, 2000: Role of sea surface temperature and soil-moisture feedback in the 1998 Oklahoma–Texas drought. *Nature*, **408**, 842–844.
- Hu, Q., and S. Feng, 2001: Variations of teleconnection of ENSO and interannual variation in summer rainfall in the central United States. *J. Climate*, **14**, 2469–2480.
- Hu, Z.-Z., and B. Huang, 2007: Dry and wet conditions in the contiguous United States: Interferential impact of ENSO and PDO. COLA Tech. Rep. 251, 30 pp.
- Huang, J., H. M. van den Dool, and K. P. Georgakakos, 1996: Analysis of model-calculated soil moisture over the United States (1931–1993) and applications to long-range temperature forecasts. *J. Climate*, **9**, 1350–1362.
- Kalnay, E., and Coauthors, 1996: The NCEP/NCAR 40-Year Reanalysis Project. *Bull. Amer. Meteor. Soc.*, **77**, 437–471.
- Klein, S. A., B. J. Sode, and N.-C. Lau, 1999: Remote sea surface temperature variations during ENSO: Evidence for a tropical atmospheric bridge. *J. Climate*, **12**, 917–932.
- Kogan, F. N., 1995: Droughts of the late 1980s in the United States as derived from NOAA polar-orbiting satellite data. *Bull. Amer. Meteor. Soc.*, **76**, 655–668.
- López-Moreno, J. I., and S. M. Vicente-Serrano, 2008: Positive and negative phases of the wintertime North Atlantic Oscillation

- and drought occurrence over Europe: A multitemporal-scale approach. *J. Climate*, **21**, 1220–1243.
- Lyon, B., and R. M. Dole, 1995: A diagnostic comparison of the 1980 and 1988 U.S. summer heat wave–droughts. *J. Climate*, **8**, 1658–1676.
- Maurer, E. P., A. W. Wood, J. C. Adam, D. P. Lettenmaier, and B. Nijssen, 2002: A long-term hydrologically based data set of land surface fluxes for the conterminous United States. *J. Climate*, **15**, 3237–3251.
- McKee, T. B., N. J. Doesken, and J. Kleist, 1993: The relationship of drought frequency and duration to time scales. Preprints, *Eighth Conf. on Applied Climatology*, Anaheim, CA, Amer. Meteor. Soc., 179–184.
- , —, and —, 1995: Drought monitoring with multiple time scales. Preprints, *Ninth Conf. on Applied Climatology*, Dallas, TX, Amer. Meteor. Soc., 233–236.
- Mo, K. C., and J. E. Schemm, 2008: Drought and persistent wet spells over the United States and Mexico. *J. Climate*, **21**, 980–994.
- , J. Nogue-Paegle, and R. W. Higgins, 1997: Atmospheric processes associated with summer floods and droughts in the central United States. *J. Climate*, **10**, 3028–3046.
- Namias, J., 1955: Some meteorological aspects of drought with specific reference to the summers of 1952–1954 over the United States. *Mon. Wea. Rev.*, **83**, 199–205.
- , 1991: Spring and summer 1988 drought over the contiguous United States—Causes and prediction. *J. Climate*, **4**, 54–65.
- Oglesby, R. J., and D. J. Erickson III, 1989: Soil moisture and the persistence of North American drought. *J. Climate*, **2**, 1362–1380.
- Paegle, J. N., K. C. Mo, and J. Bogues Paegle, 1996: Dependence of simulated precipitation on surface evaporation during the 1993 United States summer floods. *Mon. Wea. Rev.*, **124**, 345–361.
- Pal, J. S., and E. A. B. Eltahir, 2001: Pathways relating soil moisture conditions to future summer rainfall with a model of the land–atmosphere system. *J. Climate*, **14**, 1227–1242.
- Palmer, W. C., 1965: Meteorological drought. Research Paper 45, U.S. Weather Bureau, 58 pp.
- Pan, Z., M. Segal, R. Turner, and E. Takle, 1995: Model simulation of impacts of transient surface wetness on summer rainfall in the U.S. Midwest during drought and flood years. *Mon. Wea. Rev.*, **123**, 1575–1581.
- Piechota, T. C., and J. A. Dracup, 1996: Drought and regional hydrologic variation in the United States: Associations with the El Niño–Southern Oscillation. *Water Resour. Res.*, **32**, 1359–1373.
- Rajagopalan, B., E. Cook, U. Lall, and B. K. Ray, 2000: Spatiotemporal variability of ENSO and SST teleconnections to summer drought over the United States during the twentieth century. *J. Climate*, **13**, 4244–4255.
- Rayner, N. A., D. E. Parker, E. B. Horton, C. K. Folland, L. V. Alexander, D. P. Rowell, E. C. Kent, and A. Kaplan, 2003: Global analyses of sea surface temperature, sea ice, and night marine air temperature since the late nineteenth century. *J. Geophys. Res.*, **108**, 4407, doi:10.1029/2002JD002670.
- Redmond, K. T., 2002: The depiction of drought: A commentary. *Bull. Amer. Meteor. Soc.*, **83**, 1143–1147.
- Robock, A., K. Y. Vinnikov, G. Srinivasan, J. K. Entin, S. E. Hollinger, N. A. Speranskaya, S. Liu, and A. Namkhai, 2000: The global soil moisture data bank. *Bull. Amer. Meteor. Soc.*, **81**, 1281–1299.
- Ropelewski, C. F., and M. S. Halpert, 1986: North American precipitation and temperature patterns associated with the El Niño/Southern Oscillation. *Mon. Wea. Rev.*, **114**, 2352–2362.
- Schubert, S. D., M. J. Suarez, P. J. Pegion, R. D. Koster, and J. T. Bacmeister, 2004a: On the cause of the 1930s dust bowl. *Science*, **303**, 1855–1859.
- , —, —, —, and —, 2004b: Causes of long-term drought in the U.S. Great Plains. *J. Climate*, **17**, 485–503.
- , —, —, —, and —, 2008: Potential predictability of long-term drought and pluvial conditions in the United States Great Plains. *J. Climate*, **21**, 802–816.
- Seager, R., 2007: The turn of the century North American droughts: Global context, dynamics, and past analogs. *J. Climate*, **20**, 5527–5552.
- , Y. Kushnir, C. Herweijer, N. Naik, and J. Velez, 2005: Modeling of tropical forcing of persistent droughts and pluvials over western North America: 1856–2000. *J. Climate*, **18**, 4065–4088.
- , —, M. Ting, M. Cane, N. Naik, and J. Miller, 2008: Would advance knowledge of 1930s SSTs have allowed prediction of the dust bowl drought? *J. Climate*, **21**, 3261–3280.
- Smith, T. M., and R. W. Reynolds, 2004: Improved extended reconstruction of SST (1854–1997). *J. Climate*, **17**, 2466–2477.
- Ting, M., and H. Wang, 1997: Summertime U.S. precipitation variability and its relation to Pacific sea surface temperature. *J. Climate*, **10**, 1853–1873.
- Trenberth, K. E., and G. W. Branstator, 1992: Issues in establishing causes of the 1988 drought over North America. *J. Climate*, **5**, 159–172.
- , and C. J. Guillemot, 1996: Physical processes involved in the 1988 drought and 1993 floods in North America. *J. Climate*, **9**, 1288–1298.
- , G. W. Branstator, and P. A. Arkin, 1988: Origins of the 1988 North American drought. *Science*, **242**, 1640–1645.
- van den Dool, H. M., J. Huang, and Y. Fan, 2003: Performance and analysis of the constructed analogue method applied to U.S. soil moisture over 1981–2001. *J. Geophys. Res.*, **108**, 8617, doi:10.1029/2002JD003114.
- van der Schrier, G., K. R. Briffa, T. J. Osborn, and E. R. Cook, 2006: Summer moisture availability across North America. *J. Geophys. Res.*, **111**, D11102, doi:10.1029/2005JD006745.
- Wells, N., S. Goddard, and M. Hayes, 2004: A self-calibrating Palmer drought severity index. *J. Climate*, **17**, 2335–2351.
- White, W. B., A. Gershunov, and J. Annis, 2008: Climatic influences on Midwest drought during the twentieth-century. *J. Climate*, **21**, 517–531.
- Wu, W., R. E. Dickinson, H. Wang, Y. Liu, and M. Shaikh, 2006: Covariability of spring soil moisture and summertime United States precipitation in a climate simulation. *Int. J. Climatol.*, **27**, 429–438.